

Portable low-cost measurement setup for 2D imaging of organic semiconductors

Malgorzata Celuch^{#1}, Olivier Douheret[§], Przemyslaw Korpas^{*#2}, Ryszard Michnowski^{^#},
Marzena Olszewska-Placha^{#3}, Janusz Rudnicki[#]

[#]QWED Sp. z o.o., Poland

[§]Materia Nova, Belgium

^{*}Warsaw University of Technology, Institute of Radioelectronics and Multimedia Technology, Poland

[^]Vigo System S.A., Poland

¹mceluch@qwed.eu, ²p.korpas@ire.pw.edu.pl, ³m.olszewska@qwed.eu

Abstract— A portable test-fixture for the imaging of discontinuities in novel materials, such as organic semiconductors, is designed, manufactured, and validated. A 10 GHz split-post dielectric resonator (SPDR) compliant with the IEC norm is used as a microwave probe. It is built into a custom-made 2D shift-shift scanner, providing non-destructive microwave-transparent support for the sample-under-test. Microwave signal generation and measurements are performed by a new dedicated scalar network analyzer, called Q-Meter. The setup is controlled by Windows application, which allows also connecting to professional VNAs. Verification of the portable scanner is provided with respect to stand-alone SPDR and laboratory VNA. It is then applied to a PEDOT sample of current interest in organic electronics.

Keywords—material measurements, portable test-fixtures, non-destructive testing, dielectric resonators, 2D imaging, network analyzer, organic semiconductors, permittivity, dielectric loss, Gwyddion format.

I. MOTIVATION OF THE WORK

Dielectric resonator (DR) methods have already proven their usefulness and accuracy in measuring material parameters of different types of materials. In particular, the split-post dielectric resonator (SPDR) [1] is popularly applied to the extraction of dielectric constant and loss tangent of low-loss dielectrics, as standardized in the IEC norm [2], while an alternative configuration of the single-post dielectric resonator (SiPDR) [3] has been developed for resistivity measurements of semiconductors wafers as well as the surface resistance of thin resistive films.

While in case of many classical materials, the assumption of their homogeneity allows performing a single point measurement that sufficiently characterizes the material, there is a variety of novel materials, whose properties can significantly vary across their surface due to production process variations. This group includes ink-printed materials [4], 3D-printed materials [5], carbon-based polymer composites [6], or organic semiconductors [7], which exhibit a significant dependence of electromagnetic parameters on thickness non-uniformities or inhomogeneously dispersed inclusions. In such cases, reliable microwave characterization requires measuring the material parameters in a grid over the sample's surface. To this end, motorized scanners based on 5 GHz SPDRs have been

reported [8],[9], destined for laboratory use and hence driven by a fully-fledged Vector Network Analyzer (VNA). They have not been optimized for either portability, robustness, or cost.

In classical DR measurements, any VNA can be utilized, provided that it covers the required frequency range. Although professional VNAs are very accurate, they are also relatively expensive (ca. 60 k\$), bulky, and equipped with many functions redundant in DR measurements while distracting for a non-microwave-trained user. Alternative low-cost “pocket” VNAs have recently appeared on the market (e.g. [10], [11]), however, they are targeted for amateur applications and thus their operational frequency range is limited to 6 GHz (or less); moreover, adequacy of their firmware for an accurate Q-factor extraction has not been demonstrated.

In this work, we present a portable 2D imaging setup, which comprises the following original features, relevant to the needs of microwave material characterization for organic electronics:

1. A 10 GHz SPDR is chosen as a compromise between admissible sample thickness (up to 0.9 mm) and raw lateral resolution (order of 10 mm) suitable for further down-scaling with the recent methodologies of [12], [13].

2. A motorized table is designed to provide a robust and non-destructive mounting of the sample. The SPDR is built into and calibrated within the complete scanner, providing measurement transparency to the sample mounting. The details of the 2D scanner are summarized in Section II.

3. A VNA is substituted by a dedicated 10 GHz Q-Meter, a handheld device for signal generation, with firmware optimized for fast and accurate Q-factor extraction. Details of the Q-Meter are given in Section III.

4. The Q-Meter and the motorized table are controlled by a laptop application. It provides a convenient user interface with results storage in the industrial Gwyddion format [14] compatible with Open Innovation Environments such as [15].

The complete setup is manufactured at a relatively low cost (ca. 3 times of the basic SPDR price). It is affordable and easy to use for a large group of research and industrial users, including non-MW engineers, chemists or biomedical scientists, thus opening new opportunities for multidisciplinary research. An example application to an organic semiconductor sample is included in this summary and more examples (of raw and down-scaled images) will be shown at the Symposium.

II. 2D SPDR SCANNER FOR MATERIAL IMAGING

Our scanner consists of an XY-motorized table mounted under the arm holding a 10 GHz SPDR designed after [1], [2]. The whole table is moved in X-direction by a robust Standa motor [16], while a light frame of thin Teflon foil is moved in Y-direction by a Nanotec motor [17]. Typically, 1 mm or 2 mm steps are selected, though both motors allow going down to 5 micro resolution. The sample under test (SUT), once carefully placed upon the foil, remains stable and intact. A Master Unit Control Application (MUCA) allows precise positioning of the SPDR aperture over consecutive points of the 2D grid (communicating with both motors via USB) and invokes microwave measurements, by optionally, either a standard VNA (via network connection using VNA libraries) or our new Q-Meter (via USB). The readout is done through a linear frequency sweep around the expected resonance frequency in a transmission measurement, with the number of frequency points in the range of 100 - 1000. Two measurement regimes are consecutively applied at each spatial step. First, automatic frequency tracking ensures that the resonance is detected, even when material parameters rapidly change from point to point. Then, the frequency range is adjusted to approximately 3 dB band, for accurate extraction of the resonance frequency and loaded Q-factor. The measurement speed mainly depends on the microwave measuring device, as further explained.

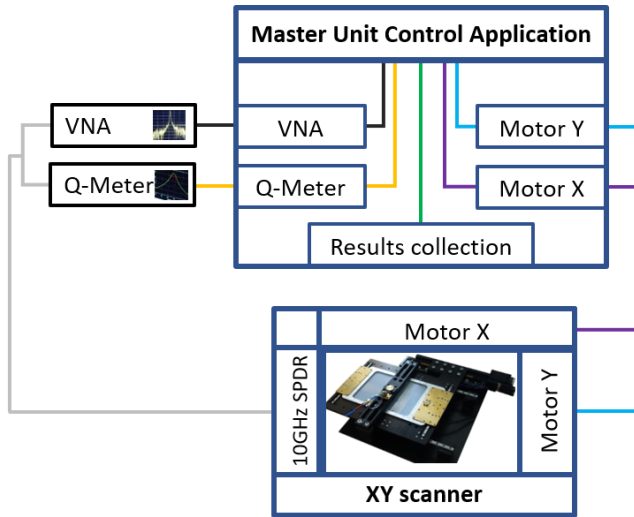


Fig. 1. Schematic of the setup MUCA with setup photo.

III. Q-FACTOR EXTRACTION DEVICE

It has previously been proven [18],[19], that an accurate Q-factor extraction can be obtained with just a scalar network analyzer. Such a device is less complicated than a vector network analyzer and can be built as a sensitive and frequency selective super-heterodyne receiver with a logarithmic RF power detector coupled together with a tracking generator (TG) [18]. This idea stands behind our custom designed Q-Meter device dedicated to operation with 10 GHz SPDRs. While the

idea is simple, the design becomes challenging, if practical constrains are taken into account:

- measurement accuracy and stability,
- dynamic range,
- cross talk between TG and receiver,
- speed of measurements,
- production-specific issues of a multilayer PCB or electronic components availability and cost.

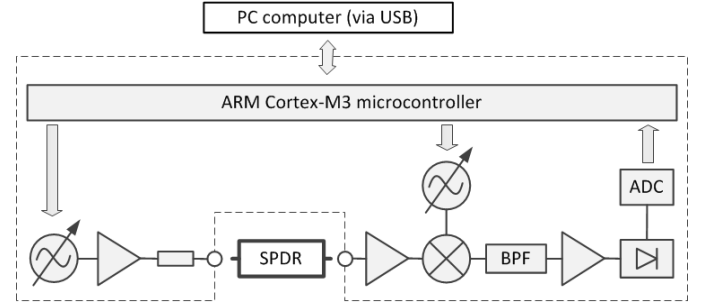


Fig. 2. A block diagram of the Q-Meter device.

The resulting Q-Meter block diagram is shown in Fig. 2. The Q-Meter extracts the quality factor of an SPDR by measuring the frequency response, in a transmission mode. For each frequency point within the required range and with an appropriate step, one port of the resonator is excited by the TG ($P_{out} \approx 0$ dBm) and a small part of this signal ($P_{in} < -40$ dBm) is transmitted to the second port of the resonator. This low power signal is captured by the receiver and its magnitude is measured on IF frequency (IF = 10.7 MHz). From those measurements, the frequency response of the resonator (module of its transmittance, $|S_{21}|$) is constructed using internally stored calibration data. Calibration in this case includes measured power levels of the TG at several frequencies and a frequency response of the RF power detector circuit. Q-factor is extracted using fast curve fitting algorithm. This algorithm provides exceptional stability of the result in comparison with a simple approach based on 3-dB marker search performed manually by the user and also implemented in many VNAs.

The dynamic range of the receiver is limited by the dynamic range of the logarithmic power detector itself (and is estimated as ca. 86dB at error below 1 dB [20]) as well as noise level, which depends on IF bandwidth. Taking into account several constrains, IF bandwidth of 180 kHz has been chosen, which results in the minimal noise floor of the receiver at approximate -110dBm.

Such a high sensitivity imposes strict requirements for electromagnetic isolation between TG and the receiver to avoid spurious cross-talks, which would be visible on measured $|S_{21}|$ characteristic and therefore affecting estimated Q-factor result. To minimize cross-talks, TG and the receiver have been physically located at opposite ends of the printed circuit board and isolated with separated chambers in a aluminum custom-milled case. Moreover, besides traditional EM gaskets use, each track on PCB, which entered isolated chamber (regardless of being data or power supply line), has been treated as a potential

path for RF leakage. As such, they have been equipped with filtering structures, which consisted of a “butterfly” and a ferrite choke, designed with the help of FDTD simulations, see Fig. 3. As a results, no cross-talks is observed above -85 dBm level, however some residual ones may still appear below this level. Such a spurious response may distract a non-MW-trained user, thereby, it has been decided to slightly decrease sensitivity from the technical limits to improve user’s experience, while keeping device fully operational (see. Fig. 3).

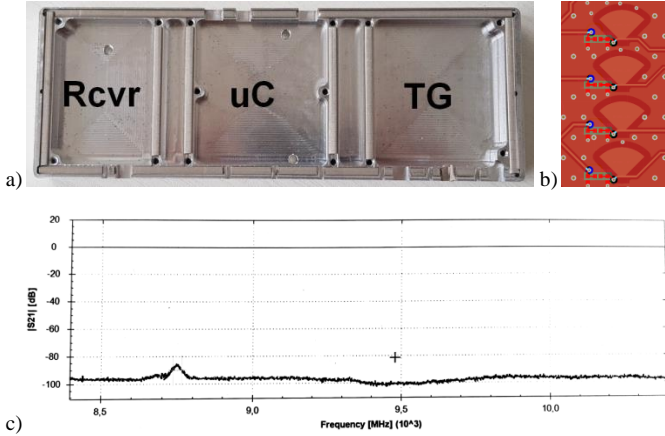


Fig. 3. Interior of the aluminum custom-milled case with isolated chambers (a), filtering structures on PCB (b) and response of the Q-Meter itself without any resonator connected (c).

For the above discussed device configuration, the measurement speed achieves ca. 3500 frequency points per second, which corresponds to about five Q-factor measurements per second, if 600 points are used to represent the $|S_{21}|$ characteristic in considered frequency band.

IV. SETUP VALIDATION ON REFERENCE SAMPLES

Validation of the new microwave setup has been performed for point-wise measurements of reference homogeneous samples including (as listed in Table 1) single-crystal quartz (black entries of Table 1) and laminate (blue). Four hardware configurations have been applied: the new scanner connected to the new Q-Meter, the same scanner connected to a laboratory VNA; then the Q-Meter and the VNA have been used in connection to a commercial stand-alone 10 GHz SPDR [21]. As shown in Table 1, the material parameters extracted by the four setups for each particular sample are within the error bounds defined by the IEC norm [2], i.e., ca. 0.3% for real permittivity and $2 \cdot 10^{-5}$ for loss tangent.

Table 1: Accuracy comparison of different characterization setups. Results are given within single-precision accuracy of the algorithm converting f and Q to material parameters (which is much better than the expected accuracy of the SPDR method, ca. 0.3% for real permittivity).

	SPDR stand-alone	SPDR in scanner
Q-Meter	3.803550-j0.000176 3.688887-j0.004745 4.365576-j0.000437	3.824762-j0.000195 3.723075-j0.004823 4.375460-j0.000523
labVNA	3.804655-j0.000139 3.698719-j0.004641 4.364580-j0.000339	3.822888-j0.000221 3.721900-j0.004417 4.374674-j0.000401

V. APPLICATION IMAGING OF ORGANIC SEMICONDUCTOR

The new scanner has been applied to samples from MateriaNova developed for organic electronics. The sample on the left of Fig. 4 is single crystal quartz substrate, purchased from Siegert Wafer (Ref. 4"/Z-Cut/500±20/DSP) and manually cleaved to cope with size dimension of the SPDR. Following a standard cleaning procedure involving successive ultrasonicated bath of soap, DI water, acetone and IPA at 60°C, a 60 nm layer of PEDOT:PSS (Poly(3,4-ethylenedioxythiophene)-poly(styrenesulfonate), Ref. Clevios PVPAl4083, Heraeus) was then deposited by spin-coating the commercial water dispersion of the material at 2000 rpm. The deposit was then backed at 120°C during 1h in an oven under primary vacuum to dry the film. The resulting PEDOT:PSS acts as a hole collecting interfacial layer in organic photovoltaic cells. The grade PVPAl 4083 and related resistivity of the material (500-5000 $\Omega \cdot \text{cm}$) was chosen to ensure sufficient shunt resistance in the device, hence its photovoltaic performances.

The lateral size of the sample is 30mm x 30mm with 0.52mm height. First, the sample has been placed approximately centrally under the SPDR head. The complex permittivity values (green in Table 1) obtained in both the new scanner and the reference commercial resonator, with both the new Q-Meter and a laboratory VNA, are in mutual agreement, and also resistivities (600-900 $\Omega \cdot \text{cm}$) in the expected resistivity range.

The sample has been imaged, with scan area enlarged to of 60mm x 60mm, so as to enclose the sample with a margin needed for further resolution enhancement by post-processing (currently under development, following [12], [13]). A scanning step of 2 mm has been used, implying 31 measurement steps in each direction and 961 total steps. The total scan time of the complete scan was 5740 seconds (1 hour 36 minutes) and the time of one measurement was 5.97 seconds. Fig. 4 shows the color-coded permittivity maps of plain quartz and PEDOT:PSS PVPAl 4083 deposited on quartz.

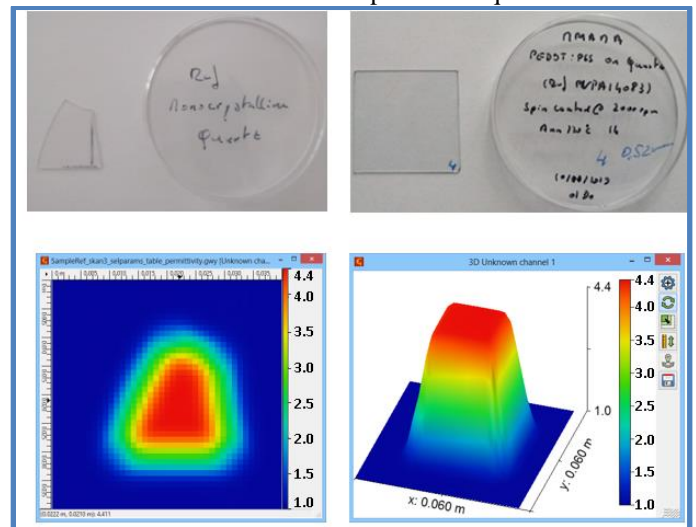


Fig. 4. Photograph of a single crystal quartz as a plain substrate (upper left) and with deposited PEDOT:PSS PVPAl 4083 (upper right) and scanned 2D maps of relative permittivity.

VI. CONCLUSIONS

In this paper a portable 2D imaging setup for microwave material characterization has been presented. The measurement setup comprises a 10 GHz SPDR, motorized table for sample placement, and handheld Q-Meter device, dedicated to fast and accurate Q-factor extraction, replacing expensive and bulky VNA. The entire measurement setup and process is conveniently controlled through laptop application, ensuring the system robustness, portability, and affordability for large group of researchers. The two main elements of the setup, SPDR scanner and Q-Meter, have been validated with reference to both, commercially available SPDR and full-scale, full-functionality laboratory VNA, proving measurements accuracy within bounds defined in IEC norm. The 2D imaging setup is then applied to characterization of an organic semiconductor sample over a grid of points, with a resolution adjusted to foreseen sample inhomogeneity. The lateral resolution of raw 2D parameters maps is limited by the diameter of dielectric resonator, being few times larger than typical scanning step. Our current research work aims at further resolution enhancement, raw 2D images are a subject of on-going research works using post-processing techniques.

ACKNOWLEDGMENT

This project has received funding from the European Union's Horizon 2020 research and innovation programme (H2020-NMBP-07-2017) under grant agreement MMAMA No. 761036.

REFERENCES

- [1] J. Krupka, A. P. Gregory, O. C. Rochard, R. N. Clarke, B. Riddle, and J. Baker-Jarvis, "Uncertainty of complex permittivity measurements by split-post dielectric resonator technique", *J. Eur. Ceramic Soc.*, vol. 21, pp. 2673-2676, 2001.
- [2] European Standard: IEC 61189-2-721:2015
- [3] J. Krupka and J. Mazierska, "Contactless measurements of resistivity of semiconductor wafers employing single-post and split-post dielectric-resonator techniques," *IEEE Trans. Instr. Meas.*, vol. 56, no. 5, pp. 1839-1844, Oct. 2007.
- [4] M. Olszewska-Placha, B. Salski, D. Janczak, P.R. Bajurko, W. Gwarek, and M. Jakubowska, "A broadband absorber with a resistive pattern made of ink with graphene nano-platelets", *IEEE Trans. Antennas and Propag.*, vol. 63, no.2, pp. 565-572, Feb. 2015.
- [5] V. Palazzi, W. Su, R. Bahr, S. Bittolo-Bon, F. Alimenti, P. Mezzanotte, L. Valentini, M. M. Tentzeris, and L. Roselli, "3D-Printing-Based Selective-Ink-Deposition Technique Enabling Complex Antenna and RF Structures for 5G Applications up to 6 GHz", *IEEE Trans. on Components, Packaging, and Manufacturing Technology*, vol. 9, no. 7, pp. 1434-1447, May 2019.
- [6] V. Kostopoulos, A. Baltopoulos, P. Karapappas, A. Vavouliotis, and A. Paipetis, "Impact and after-impact properties of carbon fibre reinforced composites enhanced with multi-wall carbon nanotubes," *Composite Science and Technology*, vol. 70, no. 4, pp. 553-563, April 2010.
- [7] O. V. Kozlov, Y.N. Luponosov, A.N. Solodukhin, B. Flament, O. Douheret, P. Viville, D. Beljonne, R. Lazzaroni, J. Cornil, S.A. Ponomarenko, and M.S. Pshenichnikov, "Simple donor-acceptor molecule with long exciton diffusion length for organic photovoltaics", *Organic Electronics*, vol. 53, pp. 185-190, Feb. 2018.
- [8] J. Krupka, D. Nguyen, and J. Mazierska, "Microwave and RF methods of contactless mapping of the sheet resistance and the complex

- permittivity of conductive materials and semiconductors," *Meas. Sci. Technol.*, vol. 22, no. 8, 085703, 2011.
- [9] J. Krupka, W. Karcz, S. P. Avdeyev, P. Kaminski, and R. Kozlowski, "Electrical properties of deuteron irradiated high resistivity silicon", *Nucl. Instr. Methods in Physics Research B*, vol. 325, pp. 107-114, 2014.
- [10] (2019) Portable Spectrum Analyzer [Online]. Available: http://www.arinst.net/arinst_ssa_tg.php
- [11] (2019) pocketVNA [Online]. Available: <https://pocketvna.com/>
- [12] P. Korpas, "Deconvolution-based spatial resolution improvement technique for resistivity scans acquired with split-post dielectric resonator", *Proc. 22nd Intl. Microwave and Radar Conf. MIKON*, pp. 541-543, Poznan, PL, May 2018.
- [13] M. Celuch, W. Gwarek, and A. Wieckowski, "Enhanced-Resolution Material Imaging with Dielectric Resonators: A New Implicit Space-Domain Technique", *IEEE MTT-S International Microwave Symposium 2019*, pp. 55-58, Boston, June 2019.
- [14] (2019) Gwyddion format documentation [Online]. Available: <http://gwyddion.net/documentation/user-guide-en/gwyfile-format.html>
- [15] (2019) MMAMA EU Horizon 2020 project website. [Online]. Available: www.mmama.eu
- [16] (2019) Standa Motor specification [Online]. Available: http://www.standa.lt/products/catalog/motorised_positioners?item=60
- [17] (2019) Nanotec Motor Controller specification [Online]. Available: <https://en.nanotec.com/products/1036-smci33-1/>
- [18] P. Korpas, L. Usydus, and J. Krupka, "Automatic Split Post Dielectric Set-up for Measurements of Substrates and Thin Conducting and Ferroelectric Films," *Ferroelectrics*, vol. 434, pp. 1-8, Jan. 2012.
- [19] J. Cuper, M. Rytel, T. Karpisz, A. Pacewicz, B. Salski, and P. Kopyt, "Ka-Band Compact Scalar Network Analyzer Dedicated to Resonator-based Measurements of Material Properties", *IEEE MTT-S International Microwave Symposium 2019*, pp. 51-54, Boston, June 2019.
- [20] Datasheet AD8306, Analog Devices.
- [21] (2019) Commercial SPDR resonators. [Online]. Available: https://qwed.eu/resonators_spdr.html